8th Australasian Congress on Applied Mechanics (ACAM 8)
CALL FOR PAPERS
ENGINEERS AUSTRALIA CONVENTION 2014
23-26 NOV MELBOURNE
ENGINEERS AUSTRALIA

Comparison Of Dynamic Stiffness And Finite Element Methods In Dynamics And Aeroelastic Response

Alfonso Pagani[1*], Marco Petrolo[2] and Erasmo Carrera[1,2]

[1] *Department of Mechanical and Aerospace Engineering, Politecnico di Torino, Italy*

[2] *School of Aerospace, Mechanical and Manufacturing Engineering, RMIT University, Australia*

[*] *Corresponding author. Email: alfonso.pagani@polito.it*

Abstract: In linear elasticity, most of the theories of structures in dynamics are governed by partial differential equations of motion. Among the others, the Finite Element Method (FEM) is a numerical technique aiming at solving the above problem by reducing it in a system of algebraic equations. Although being very popular, FEM suffers of some well-known problems and it is limited to the low-frequency range. An alternative method is the Dynamic Stiffness Method (DSM), which allows to solve the differential equations of motion in an exact manner with no numerical approximations. DSM has most of the FEM capabilities. However, unlike FEM, DSM brings to a transcendental non-linear eigenvalue problem and the algorithm by Wittrick and Williams, which is an iterative procedure, is needed to solve the frequency-dependant Dynamic Stiffness matrix. In this work, FEM and DSM are applied with reference to the Carrera Unified Formulation (CUF), which allows for the straightforward implementation of higher-order hierarchical beam theories without the need for ad hoc assumptions. Different structural problems are addressed, including metallic and composite lifting surfaces for free vibrations and aeroelastic response analyses. The results show the uncompromising accuracy of DSM in seeking the free vibration characteristics of the structures considered. On the other hand, it is demonstrated that FEM is sufficient for flutter analysis since aeroelastic phenomena only excite the first vibration modes.

Keywords: aeroelasticity, beams, Carrera unified formulation, doublet lattice method, dynamic stiffness method, finite element method, flutter.

1 Introduction

Aeroelasticity plays a critical role in the design of modern aerospace vehicles. Among others, flutter is one of the most important aeroelastic phenomena. Flutter can occur to a structure in a flow field, and it consists of undamped vibrations that can lead to catastrophic collapses. Different analysis tools have been developed to predict flutter after the publication of the now famous report by Theodorsen [1], nearly 80 years ago. The doublet lattice method (DLM) emerged in the late 1960s [2]. In the present work, an improved version of DLM, which was recently proposed by Rodden et al. [3], has been coupled with a refined one-dimensional (1D) structural formulation for the flutter analysis of both isotropic and composite lifting surfaces.

Refined beam models are developed within the framework of the Carrera Unified Formulation (CUF), which is well established in the literature for over a decade [4]. CUF is a hierarchical formulation that considers the order of the model, N, as a free-parameter (i.e. as an input) of the analysis or in other words, refined models are obtained without having the need for any ad hoc formulations. In the present work, beam theories using CUF [5] are obtained on the basis of Taylor-type expansions (TE). Classical models (Euler-Bernoulli, EBBT, and Timoshenko beam theories, TBT) can be obtained as particular cases. The strength of CUF TE 1D models in dealing with arbitrary geometries, thin-walled structures and identifying local effects are well known for both static [6] and free-vibration analysis [7].

In majority of the papers on 1D CUF, the finite element method (FEM) has been used to handle arbitrary geometries and loading conditions. Recently, a new approach for CUF TE theories through the application of the dynamic stiffness method (DSM) was provided and applications to free vibration analysis of isotropic [8] and composite [9] beams revealed the strength of this methodology. In the present paper, both FEM and DSM are used to solve the equations of motion coming from CUF TE refined beam models and free vibration characteristics of both metallic and laminated lifting surfaces are evaluated. The results from modal analyses by FEM and DSM are compared and the mode shapes are used with reference to DLM to carry out flutter analyses [10-12].

The application of FEM to CUF models is not provided here for the sake of brevity, however a detailed dissertation can be found in [13]. On the other hand, the extension of DSM to refined beam CUF models is briefly outlined hereinafter. The paper is organized as follows: (i) first CUF is introduced and higher-order models are formulated, (ii) secondly, the principle of virtual displacements is used to derive the differential governing equations and the associated natural boundary conditions, (iii) next, the DSM is briefly discussed, (iv) both FEM and DSM are then used to compute the natural frequencies and mode shapes of metallic and composite lifting surfaces and, (v) finally, flutter analyses are carried out through DLM and g-method [14].

2 Governing equations of the *N*-order beam model by CUF

The adopted rectangular Cartesian coordinate system is shown in Figure 1: . The cross-section of the beam lies on the xz-plane and it is denoted by Ω, whereas the boundaries over y are $0 \leq y \leq L$. Let us introduce the transposed displacement vector,

$$\boldsymbol{u}(x,y,z;t) = \{u_x \; u_y \; u_z\}^T \tag{1}$$

Within the framework of the CUF, the 3D displacement field (1) is expressed as

$$\boldsymbol{u}(x,y,z;t) = F_\tau(x,z)\boldsymbol{u}_\tau(y;t), \qquad \tau = 1,2,\dots,M \tag{2}$$

Where F_τ are the functions of the coordinates x and z on the cross-section. $\boldsymbol{u}_\tau$ is the vector of the generalized displacements, M stands for the number of the terms used in the expansion, and the repeated subscript, τ indicates summation. TE (Taylor Expansion) 1D CUF models consist of McLaurin series that uses the 2D polynomials $x^i z^j$ as F_τ functions, where i and j are positive integers.

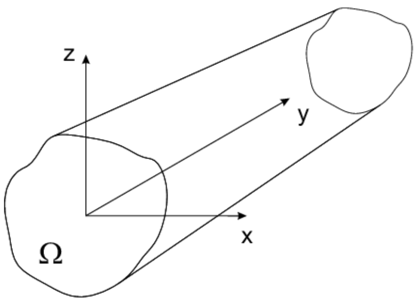

Figure 1: Coordinate frame of the beam model

In this paper, the principle of virtual displacement is used to derive the equations of motion.

$$\delta L_{int} = \int_V \delta\boldsymbol{\epsilon}^T \boldsymbol{\sigma} \, dV = -\delta L_{ine} \tag{3}$$

Where $\boldsymbol{\epsilon}$ and $\boldsymbol{\sigma}$ are the strain and stress vectors, respectively. δL_{int} stands for the strain energy and

δL_{ine} is the work done by the inertial loadings. δ stands as usual virtual variation operator. The virtual variation of the strain energy is rewritten using (2), the constitutive laws, and the linear strain-displacement relations. After integrations by part, (3) becomes

$$\delta L_{int} = \int_L \delta \boldsymbol{u}_\tau^T \, \boldsymbol{K}^{\tau s} \, \boldsymbol{u}_s \, dy + [\delta \boldsymbol{u}_\tau^T \, \boldsymbol{\Pi}^{\tau s} \, \boldsymbol{u}_s]_{y=0}^{y=L} \tag{4}$$

where $\boldsymbol{K}^{\tau s}$ is the differential linear stiffness matrix and $\boldsymbol{\Pi}^{\tau s}$ is the matrix of the natural boundary conditions in the form of 3×3 fundamental nuclei. The components of the nuclei are not given in the present work for the sake of brevity. They can be found in [8, 9]. The virtual variation of the inertial forces is also rewritten in terms of the fundamental nucleus.

$$\delta L_{ine} = \int_L \delta \boldsymbol{u}_\tau \int_\Omega \rho \, F_\tau \, F_s \, d\Omega \, \ddot{\boldsymbol{u}}_s \, dy = \int_L \delta \boldsymbol{u}_\tau \, \boldsymbol{M}^{\tau s} \, \ddot{\boldsymbol{u}}_s \, dy \tag{5}$$

Where ρ is the material density and $\boldsymbol{M}^{\tau s}$ is the fundamental nucleus of the mass matrix. Double over dots stand as second derivative with respect to time (t).

In the case of harmonic motion, $\boldsymbol{u}_s(y;t) = \boldsymbol{U}_s(y) \, e^{i\omega t}$, the equations of motion can be expressed as follows:

$$\delta \boldsymbol{U}_\tau\!: \quad \boldsymbol{L}^{\tau s} \, \widetilde{\boldsymbol{U}}_s = 0 \tag{6}$$

Where the vector $\widetilde{\boldsymbol{U}}_s$ contains the amplitudes of the harmonically varying generalized displacements and their first and second derivatives. $\boldsymbol{L}^{\tau s}$ is the 3×9 matrix that contains the coefficients of the ordinary differential equations. Its components are not give here for the sake of brevity, but they can be found in [8, 9]. For a given expansion order N, the equations of motion of the generic beam theory can be obtained by expanding (6) for τ and s ranging from 1 to $M = (N+1)(N+2)/2$. In a similar way, the boundary conditions can be written in a matrix form as

$$\delta \boldsymbol{U}_\tau\!: \quad \boldsymbol{P}_s = \boldsymbol{B}^{\tau s} \, \widehat{\boldsymbol{U}}_s \tag{7}$$

where $\boldsymbol{P}_s$ is the generalised loading vector and $\widehat{\boldsymbol{U}}_s$ contains the amplitudes of the harmonically varying generalized displacements and their first derivatives. $\boldsymbol{B}^{\tau s}$ is the 3×6 matrix that contains the coefficient of the natural boundary conditions (see [8, 9]) and it has to be expanded according to N in the same way of the $\boldsymbol{L}^{\tau s}$ matrix.

3 Dynamic Stiffness Method

The present free vibration problem is described by a system of ordinary differential equations (ODEs) of second-order in y with constant coefficients. A change of variables is used to reduce the second order system of ODEs to a first-order system,

$$\boldsymbol{Z} = \{Z_1 \;\; Z_2 \;\; \ldots \;\; Z_n\}^T = \widehat{\boldsymbol{U}} \tag{8}$$

Where $\widehat{\boldsymbol{U}}$ is the expansion of $\widehat{\boldsymbol{U}}_s$. In [8], an automatic algorithm to transform the expanded $\boldsymbol{L}$ matrix of (6) into the matrix $\boldsymbol{S}$ of the following linear differential system was described:

$$\boldsymbol{Z}_{,y}(y) = \boldsymbol{S} \, \boldsymbol{Z}(y) \tag{9}$$

Once the differential problem is expressed in terms of (9), the solution can be written as follows:

$$\boldsymbol{Z} = \boldsymbol{\delta}\, \boldsymbol{C}\, e^{\boldsymbol{\lambda} y} \tag{10}$$

Where $\boldsymbol{\lambda}$ is the vector of the eigenvalues of $\boldsymbol{S}$. The element δ_{ij} of matrix $\boldsymbol{\delta}$ is the j[th] component of the i[th] eigenvector of matrix $\boldsymbol{S}$ and the vector $\boldsymbol{C}$ contains the integration constants that need to be determined by using the boundary conditions. By evaluating (10) in $y = 0$ and $y = L$, and by applying the boundary conditions (7), the following matrix relation for the nodal displacements is obtained:

$$\overline{\boldsymbol{U}} = \boldsymbol{A}\, \boldsymbol{C} \tag{11}$$

Similarly, boundary conditions for generalized nodal forces are written as follows:

$$\overline{\boldsymbol{P}} = \boldsymbol{R}\, \boldsymbol{C} \tag{12}$$

$\overline{\boldsymbol{U}}$ and $\overline{\boldsymbol{P}}$ are the vectors of the amplitudes of the harmonically varying nodal generalized displacements and loads, respectively. The constant vector $\boldsymbol{C}$ from (11) and (12) can now be eliminated to give the DS matrix of the element as follows

$$\overline{\boldsymbol{P}} = \boldsymbol{\mathcal{K}}\, \overline{\boldsymbol{U}} \tag{3}$$

Where $\boldsymbol{\mathcal{K}}$ is the required frequency dependant DS matrix. The DS matrix given above is the basic building block to compute the exact natural frequencies of a higher-order beam. It is possible to assemble elemental DS matrices to form the overall DS matrix of any complex structures consisting of beam elements. Once the global DS matrix of the final structure is obtained, the boundary conditions can be applied by using the well-known penalty method. For free vibration analysis of structures, FEM generally leads to a linear eigenvalue problem. By contrast, the DSM leads to a transcendental (non-linear) eigenvalue problem for which the Wittrick-Williams algorithm [15] is recognisably the best available solution technique at present. Further details about the computation of the natural frequencies and the mode shapes can be found in [8].

4 Doublet Lattice Method

Following [16] or [2], the normalwash in a point with coordinates x, y due to the pulsating pressure jump $\overline{\Delta p}$ in the point ξ, η has the following expression:

$$\overline{w} = \frac{1}{8\pi}\int_A \overline{\Delta p}\;\; K(x_0, y_0, \omega, M) dA \tag{14}$$

Where M is the Mach number, ω is the circular frequency, and $x_0 = x - \xi,\ y_0 = y - \eta$. The kernel function ($K$) formal expression is not reported here for the sake of brevity, it can be found in [16]. (14) can be numerically solved by means of the Doublet Lattice Method (DLM). In the DLM framework, a lifting surface is discretized in a number of panels and the following algebraic system of equations has to be solved:

$$\overline{w}_i = \sum_{j=1}^{N_{AP}} D_{ij} \overline{\Delta p}_j \tag{15}$$

Where N_{AP} indicates the total number of aerodynamic panels and D_{ij} is the normal wash factor. In this paper D_{ij} was calculated by exploiting Rodden's quartic DLM [3]. For the sake of brevity, the procedure to compute the normalwash factor is not reported here, it can be found in the Rodden's paper. It is important to underline that the steady contribution to D_{ij} was computed via the Vortex Lattice Method (VLM) [17]. On the other hand, the unsteady aeroelastic analysis was carried out by considering a set of modal shapes as generalized motions for the unsteady aerodynamic generalized force generation [10-12].

The generalized aerodynamic matrix for a given reduced frequency (k) is given by

$$Q_{ij}(ik) = \sum_{N=1}^{N_{AP}} \Delta p_j^N(ik)\, \tilde{\mathcal{Z}}_{\mathrm{i}}^{\,N}\, A^N \tag{16}$$

Where

- $k = \omega b/L$, b is the reference length (equal to the half of the reference chord) and L is the length of the structure.
- $\Delta p_j^N(ik)$ is the pressure jump due to the j-th set of motions (modal shapes), acting on the N-th aerodynamic panel and evaluated for a given reduced frequency. The computation of the pressure jump is performed by means of the DLM.
- $\tilde{\mathcal{Z}}_{\mathrm{i}}^{\,N}$ is the i-th motion set evaluated at the N-th aerodynamic panel. Starting from the i-th modal shape given by a structural model, the i-th motion set is then mapped on the aerodynamic panels by means of the splining process. In this work, modal shapes were evaluated by means of CUF 1D models and both FEM and DSM as solution procedures.
- A^N is the area of the N-th panel.

$\boldsymbol{Q}(ik)$ is a square matrix with $N_{modes} \times N_{modes}$ elements, where N_{modes} indicates the total number of natural modes adopted. Typically, N_{modes} ranges from 10 to 20.

The g-method, which was introduced by Chen [14], is used in this paper to solve the flutter problem. The basic assumption of the g-method is based on the following approximation of the generalized aerodynamic matrix:

$$\widetilde{\boldsymbol{Q}}(p) \approx \widetilde{\boldsymbol{Q}}(ik) + g\widetilde{\boldsymbol{Q}}'(ik), \quad \text{for} \quad g \ll 1 \tag{17}$$

Where g = γk and γ is the transient decay rate coefficient. Equation (17) leads to the g-method equation:

$$\left[\left(\frac{V_\infty}{b}\right)^2 \widetilde{\boldsymbol{M}}p^2 + \widetilde{\boldsymbol{K}} - \frac{1}{2}\rho V_\infty^2 \widetilde{\boldsymbol{Q}}'(ik)g - \frac{1}{2}\rho V_\infty^2 \widetilde{\boldsymbol{Q}}(ik)\right]\{\boldsymbol{q}(p)\} = 0 \tag{18}$$

Where $\widetilde{\boldsymbol{M}}$ and $\widetilde{\boldsymbol{K}}$ are the generalized mass and stiffness matrices, p is the nondimensional Laplace parameter (p = g + ik), and b is is the reference length (usually equal to the half of the reference chord). The generalized aerodynamic matrix, $\widetilde{\boldsymbol{Q}}(ik)$, is provided by the unsteady aerodynamic model (DLM) in the frequency domain. The computation of $\widetilde{\boldsymbol{Q}}'(ik)$ has to be performed numerically. (18) can be written in the following form:

$$[g^2\boldsymbol{A} + g\boldsymbol{B} + \boldsymbol{C}]\{\boldsymbol{q}\} = 0 \tag{19}$$

This is a second-order linear system in g. The g-method targets to find those solutions having $Im(g) = 0$. A so-called *reduced-frequency-sweep technique* is adopted to find a sign change of the imaginary part of each eigenvalue in a range of k values. If the sign change occurs and $Re(g) > 0$, the reduced flutter frequency is then computed by means of a linear interpolation.

5 Numerical Results

Numerical assessments were carried out on isotropic and composite structures. Figure 2 shows the sweep and fiber orientation angles (positive directions). An 8×30 aerodynamic mesh was exploited and the first ten natural modes were used to build the generalized matrices.

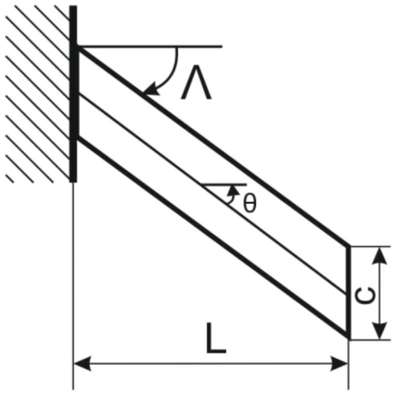

Figure 5: Sweep and fiber orientation angles

5.1 Isotropic plate wing

An isotropic wing modeled as a flat plate was first considered. The wing model that was investigated has the following characteristics: $L = 0.305$ m, $c = 0.076$ m, and thickness $t = 0.001$ m. The material is an aluminum alloy with elastic modulus $E = 73.8$ GPa, shear modulus $G = 27.6$ GPa and density $\rho = 2768\ \mathrm{Kg}/m^3$. This model was retrieved from [18].

Table 1 shows the first three natural frequencies for a swept back configuration (Λ = 30°). Different beam models were considered, classical (EBBT and TBT) and CUF higher-order (from N = 1 to N = 4). The results that were obtained through both FEM and DSM approaches. Bending and torsional modes were detected.

Table 1: Effect of the CUF 1D expansion order (N) on the vibration frequencies (Hz) of the isotropic plate wing by means of DSM and FEM, Λ = 30°

Model	Method	f_1	f_2	f_3
EBBT	FEM	8.967	56.192	157.335
	DSM	8.968	56.191	157.336
TBT	FEM	8.966	56.189	157.320
	DSM	8.967	56.190	157.320
N = 1	FEM	8.966	56.185	157.308
	DSM	8.965	56.186	157.308
N = 2	FEM	7.199	44.462	97.939*
	DSM	7.180	44.338	97.863*
N = 3	FEM	7.125	43.778	74.316*
	DSM	7.105	43.654	74.412*
N = 4	FEM	7.093	43.529	73.296*
	DSM	7.070	43.389	73.370*

*Torsional mode

Table 2 shows the flutter velocity of the forward swept configuration (Λ = -30°). Again, the DSM was compared against FEM [10] and the influence of the beam model was evaluated. The results from the classical and the linear (N = 1) models were not reported since no flutter conditions were detected by those models. In fact, as it is clear from Table 1, the classical and the linear (N = 1) structural models are not able to foresee torsion and coupling phenomena, which are fundamental in flutter analysis.

5.2 Composite plate wing

In the second analysis case, composite wing structures were considered. Composite plate wing models were retrieved from [19, 20]. A graphite/epoxy composite material with the following characteristics was used: $E_L = 98.0\ GPa$, $E_T = 7.90\ GPa$, $G_{LT} = 5.60\ GPa$, Poisson ratio $\nu = 0.28$ and $\rho = 1520\ \mathrm{Kg}/m^3$, where L denotes the fibers direction and T a direction perpendicular to the fibers. The length of the wing (L) is equal to 305 mm and the chord (c) is equal to 76.2 mm. The total thickness of the laminate is 0.804 mm.

Table 2: Effect of the CUF 1D expansion order (N) on the flutter velocities of the isotropic plate wing by means of DSM and FEM, Λ = -30°

Model	Method	Velocity (m/s)
N = 2	FEM	84.206
	DSM	84.086
N = 3	FEM	59.202
	DSM	59.366
N = 4	FEM	58.050
	DSM	58.188

Symmetric six-layer laminates with constant thickness layers were considered. The plate wing was straight (Λ = 0°). Table 6 shows the flutter velocities for various stacking sequences and various beam models. DSM was used in this analysis and the results were compared with those from CLT (Classical Laminate Theory) plate models and with experimental results from the literature.

Table 3: Flutter velocities (m/s) for a six-layer straight plate wing. DSM CUF beam vs CLT [19] and experiments [20]

Stacking	N = 2	N = 3	N = 4
$[0_2/90]_s$ CLT, 23.0 EXP, 25	23.3	23.3	23.2
$[45/-45/0]_s$ CLT, 40.1 EXP, > 32	43.3	40.4	40.4
$[45_2/0]_s$ CLT, 27.5 EXP, 28	32.5	26.9	26.7
$[30_2/0]_s$ CLT, 27.1 EXP, 27	29.3	26.3	26.3

6 Conclusions

In this paper both FEM and DSM have been exploited to solve governing equations of refined CUF beam models and to carry out free vibration analyses of isotropic and composite plate wings. The results have been then used with reference to DLM and g-method to detect the flutter conditions. The conducted anayses draw the following conclusions:

- CUF is a very powerful tool to analyze the free vibration characteristics of isotropic and composite structures.
- As far as flutter analyses are concerned, the present 1D approach provides results that perfectly match those ones from 2D FEM and experiments.
- The adoption of refined beam models is compulsory to detect flutter. This is due to the influence of the bending-torsion coupling.
- DSM is an exact method to solve the present refined CUF models. However, FEM still yields acceptable results for both free vibration and flutter analyses.

References

1. T. Theodorsen, 1934, “General theory of aerodynamic instability and the mechanism of flutter”, *NACA Rept*. 496.
2. E. Albano and W.P. and Rodden, 1969, “A doublet-lattice method for calculating lift distributions on oscillating surfaces in subsonic flows”, *AIAA Journal*, vol. 7, no. 2, pp. 279-285.

3. W.P. Rodden, P.F. Taylor and S.C.J. McIntosh, 1998, “Further refinement of the subsonic doublet-lattice method”, *Journal of Aircraft*, vol. 35, no. 5, pp. 720-726.

4. E. Carrera, 1995, “A class of two dimensional theories for multilayered plates analysis”, *Atti Accademia delle Scienze di Torino, Memorie Scienze Fisiche*, vol. 19-20, pp. 49-87.

5. E. Carrera, G. Giunta and M. Petrolo, 2011, *Beam Structures: Classical and Advanced Theories*, John Wiley & Sons.

6. E. Carrera, M. Petrolo and E. Zappino, 2012, “Performance of CUF approach to analyze the structural behavior of slender bodies”, *Journal of Structural Engineering*, vol. 138, pp. 285-297.

7. M. Petrolo, E. Zappino and E. Carrera, 2012, “Refined free vibration analysis of one-dimensional structures with compact and bridge-like cross-sections”, *Thin-Walled Structures*, vol. 56, pp. 49-61.

8. A. Pagani, M. Boscolo, J.R. Banerjee and E. Carrera, 2013, “Exact dynamic stiffness elements based on one dimensional higher-order theories for free vibration analysis of solid and thin-walled structures”, *Journal of Sound and Vibration*, vol. 332, no. 23, pp. 6104-6127.

9. A. Pagani, E. Carrera, M. Boscolo and J.R. Banerjee, 2014, “Refined dynamic stiffness elements applied to free vibration analysis of generally laminated composite beams with arbitrary boundary conditions”, *Composite Structures*, vol. 110, pp. 305-316.

10. M. Petrolo, 2012, “Advanced 1D structural models for flutter analysis of lifting surfaces”, *International Journal of Aeronautical and Space Sciences*, vol. 13, no. 2, pp. 199-209.

11. M. Petrolo, 2013, “Flutter analysis of composite lifting surfaces by the 1D Carrera unified formulation and the doublet lattice method”, *Composite Structures*, vol. 95, no. 8, pp. 539-546.

12. A. Pagani, M. Petrolo and E. Carrera, 2014, “Flutter analysis by refined 1D dynamic stiffness elements and doublet lattice method”, Advances in Aircraft and Spacecraft Science, vol. 1, no. 3, pp. 291-310.

13. E. Carrera, M. Cinefra, M. Petrolo and E. Zappino, 2014, *Finite Element Analysis of Structures through Unified Formulation*, John Wiley & Sons.

14. P.C. Chen, 2000, “Damping perturbation method for flutter solution: the g-method”, *AIAA Journal*, vol. 38, no. 9, pp. 1519-1524.

15. W.H. Wittrick and F.W Williams, 1970, “A general algorithm for computing natural frequencies of elastic structures”, *Quarterly Journal of Mechanics and Applied Sciences*, vol. 24, no. 3, pp. 263-284.

16. M.T. Landahl, 1967, “Kernel function for nonplanar oscillating surfaces in a subsonic flow”, *AIAA Journal*, vol. 5, no. 5, pp. 1045-1046.

17. J. Katz and A. Plotkin, 1991, *Low-Speed Aerodynamics: From Wing Theory to Panel Methods*, McGraw-Hill, Inc., New York.

18. K.N. Koo, 2001, “Aeroelastic Characteristics of Double-Swept Isotropic and Composite Wings” , *Journal of Aircraft*, vol. 38, no. 2, pp. 343-348.

19. M. Kameyama and H. Fukunaga, 2007, “Optimum design of composite plate wings for aeroelastic characteristics using lamination parameters”, *Computers and Structures*, vol. 85, pp. 213-224.

20. S.J. Hollowell and J. Dugundji, 1984, “Aeroelastic flutter and divergence of stiffness coupled, graphite/epoxy cantilevered plates”, *Journal of Aircraft*, vol. 21, no. 1, pp. 69-76.